Elsevier Editorial System(tm) for Journal of Hydrology
Manuscript Draft

Manuscript Number: HYDROL8482R1

Title: Estimating rainfall erosivity from daily precipitation records: a comparison among methods using data from the Ebro Basin (NE Spain)

Article Type: Research Paper

Keywords: rainfall erosivity; RUSLE R factor; daily rainfall erosivity models; modified Fournier index; Ebro basin; NE Spain

Corresponding Author: Miss Marta Angulo-Martínez, Ph.D

Corresponding Author's Institution: Experimental Station Aula Dei

First Author: Marta Angulo-Martínez

Order of Authors: Marta Angulo-Martínez; Santiago Beguería

Estimating rainfall erosivity from daily precipitation records: a comparison among methods using data from the Ebro Basin (NE Spain)

M. Angulo-Martínez[1*], S. Beguería[1]

[1] {Department of Soil and Water, Aula Dei Experimental Station–CSIC. 1005 Avda. Montañana, 50080–Zaragoza (Spain). Tlf: (+34) 976 716 158; Fax: (+34) 976 716 145}

Correspondence to: M. Angulo-Martínez (mangulo@eead.csic.es)

Abstract

Among the major factors controlling soil erosion, as vegetation cover or soil erodibility, rainfall erosivity has a paramount importance since it is difficult to predict and control by humans. Accurate estimation of rainfall erosivity requires continuous rainfall data; however, such data rarely demonstrate good spatial and temporal coverage. Daily weather records are now commonly available, providing good coverage that better represents rainfall intensity behavior than do more aggregated rainfall data. In the present study annual rainfall erosivity was estimated from daily rainfall records, and compared to data obtained employing the RUSLE *R* factor procedure. A spatially-dense precipitation database of high temporal resolution (15 min) was used. Two methodologies were applied: i) daily rainfall erosivity estimated using several parametric models, and, (ii) annual rainfall erosivity estimated by regression-based techniques employing several intensity precipitation indices and the modified Fournier index. To determine the accuracy of estimates, several goodness-of-fit and error statistics were computed in addition to a spatial distribution comparison. The daily rainfall erosivity models accurately predicted annual rainfall erosivity. Parametric models with few combined parameters and a periodic function simulating intra-annual rainfall behavior provided the best results. Where daily rainfall records were not available, good estimates of

annual rainfall erosivity were also obtained using regression-based techniques based on 5-day maximum precipitation events, the maximum wet spell duration, and the ratio between the lengths of average wet and dry spells. Inherent limitations remain in the use of daily weather records for estimating rainfall erosivity. Future research should focus on incorporating measures of natural rainfall properties of the particular region, including kinetic energy and intensity, and their effects on the soil.

Keywords: rainfall erosivity; RUSLE *R* factor; daily rainfall erosivity models; modified Fournier index; Ebro basin; NE Spain

1. Introduction

Rainfall erosivity is of paramount importance among natural factors affecting soil erosion, and unlike some other natural factors, such as relief or soil characteristics, is not amenable to human modification. It thus represents a natural environmental constraint that limits and conditions land use and management. In the context of climate change the effect of altered rainfall characteristics on soil erosion is one of the main concerns of soil conservation studies.

It is well known that several very intense rainfall events are responsible for the largest proportion of soil erosion and sediment delivery. Hence, estimating rainfall erosivity is central to assessment of soil erosion risk. Numerous studies using natural and simulated rainfall have investigated the role of drop size distribution on the detachment of soil particles. The measurements involved are difficult to perform, and reported data are consequently very limited both spatially and temporally. In addition, measurements of natural rainfall properties, for comparison with simulated rain, are scarce (Dunkerley 2008). This has encouraged studies relating more conventional rainfall indices, such as the maximum intensity during a period of time, to overall rainfall energy or directly to soil detachment rates. Examples of such indices

of rainfall erosivity are the USLE *R* factor, which summarizes all the erosive events quantified by the EI_{30} index occurred along the year (Wischmeier 1959, Wischmeier and Smith 1978, Brown and Foster 1987), the modified Fournier index for Morocco (Arnoldus 1977), the KE > 25 index for southern Africa (Hudson 1971), and the AIm index for Nigeria (Lal 1976). Among these the most extensively used is the USLE/RUSLE *R* factor, which is calculated from the EI_{30} index (Wischmeier 1959, Wischmeier and Smith 1978, Brown and Foster 1987, Renard *et al.* 1996). At many sites worldwide the *R* factor has been shown to be highly correlated with soil loss (Van der Knijff et al. 2000, Diodato 2004, Shi et al. 2004, Hoyos et al. 2005, Curse et al. 2006, Onori et al. 2006, Domínguez-Romero et al. 2007).

One of the main disadvantages in seeking to employ the RUSLE *R* factor is the need for a relatively continuous rainfall data series, with a time resolution of at least 15 min (pluviograph data). Information of this nature is rarely available with good spatial and temporal coverage. Other attempts to predict rainfall erosivity from mean annual rainfall and/or mean monthly rainfall have provided results that are quite coarse, but these have been extensively cited in the scientific literature (Banasik and Górski 1994, Renard and Freimund 1994, Yu & Rosewell 1996c, Ferro et al. 1999). Renard and Freimund (1994) provided a succinct summary of methods for estimating the *R* factor in various parts of the world, and also developed a new set of relationships for calculating the *R* factor using mean annual rainfall data and the modified Fournier index.

Daily weather records with good spatial and temporal coverage that adequately represent rainfall characteristics are usually available for most locations. Because of the high temporal and spatial variability of rainfall erosivity, accurate records based on long data series are required. Attempts to accurately predict rainfall erosivity from daily rainfall records or storm events (Richardson et al. 1983, Bagarello and D'Assaro 1994, Petkovsek and Mikos 2004), or from monthly rainfall (Yu and Rosewell 1996a, b and c, Yu et al. 2001), have been based largely on exponential relationships.

As the origin of rainfall erosivity is linked to climate dynamics, there is a need to apply climate analysis methodologies to the study of the erosivity factor. However, long series of rainfall erosivity data are required if consistent results are to be obtained. Daily rainfall erosivity models bridge the gap between climate change scenarios based on general and regional circulation models, and the implications of these scenarios for some land degradation processes (Yu and Rosewell 1996b). In addition, a daily rainfall erosivity model would have potential application in many erosion constructs, as the daily model would provide robust predictions of rainfall erosivity.

The aim of this study was to review existing methodologies for predicting the *R* factor, and to compare estimates obtained using these methodologies with *R* factor values calculated by the RUSLE procedure. The study was conducted using data from a dense network of observatories distributed in a climatically complex region (the Ebro Basin, NE Spain), and covers the period 1997–2006. The methodology described has the potential to be applied to longer daily rainfall data bases, which could improve estimates of the spatial coverage of rainfall erosivity in the Ebro Basin with respect to both long-term average erosivity and seasonal distribution thereof. The proposed methodology can be applied in many parts of the world where short time series of high-resolution rainfall data coexist with long series at a daily resolution.

2. Materials and Methods

2.1. Study area

The study area covers northeastern Spain (Figure 1), encompassing an area of about 85,000 km^2 that corresponds to the Ebro Basin. The Ebro valley is an inner depression surrounded by high mountain ranges. It is limited in the north by the Cantabrian Range and the Pyrenees, with maximum elevations above 3000 m a.s.l. The Iberian Range closes the Ebro valley to the south, with maximum elevations in the range 2000–2300 m a.s.l. The Ebro valley is closed to the east by the Catalan Prelittoral Range, with maximum elevations of 1000–1900 m a.s.l.

105 The climate is influenced by the Cantabric and Mediterranean seas, and the effect of the relief
106 on precipitation and temperature. The bordering mountain ranges isolate the central valley,
107 blocking the maritime influence and resulting in a continental climate with arid conditions
108 (Cuadrat 1991, Lana and Burgueño 1998, Creus 2001, Vicente-Serrano 2005). A climatic
109 gradient in the NW–SE direction is notable, determined by the strong Atlantic Ocean
110 influences in the north and northwest of the area during much of the year, and the influence of
111 the Mediterranean Sea to the east. The mountain ranges add complexity to the climate of the
112 region. The Pyrenees extend the Atlantic Ocean influence to the east by increasing
113 precipitation.

114 The precipitation regime shows strong seasonality (Garrido and García 1992) involving both
115 the amount of precipitation and its precipitation mechanisms (frontal or convective).
116 Precipitation in inland areas is characterized by alternating wet and dry periods as a
117 consequence of the seasonal displacement of the polar front and its associated pressure
118 systems. Inter-annual variability in precipitation can be very high, and prolonged dry periods
119 can be followed by torrential rainfall events that last for many days (Martín-Vide 1994).

120 Close to the Mediterranean Sea the amount of precipitation also increases as a consequence of
121 the maritime influence. Nevertheless, the precipitation frequency, intensity and seasonality
122 close to the Mediterranean Sea are very different from areas at the north-east where
123 precipitation is frequent but rarely very intense (García-Ruiz et al. 2000). The most extreme
124 precipitation events have been recorded along the Mediterranean seaside (Romero et al. 1998,
125 Llasat 2001, Peñarrocha et al. 2002). Due to its complex climatology (as a consequence of
126 being a meteorological border region) and the contrasted relief, the Ebro Basin has a long
127 history of social, economic and environmental damage caused by extreme rainfall events
128 (García-Ruiz et al. 2000, Lasanta 2003, Llasat et al. 2005).
129

130 **2.2. Database**

The database consisted of 111 selected rainfall series from the Ebro Hydrographical Confederation automatic hydrological information network system (SAIH; Figure 1). Each station provides precipitation data at a time resolution of 15 min. The system started in 1997, and is the only dense network in the region providing sub-daily resolution data. We used all available data series for the period 1 January 1997 to 31 December 2006.

The rainfall series were subjected to a quality control process that identified incorrect records due to system failures. These records were replaced with corresponding values from a nearby station. This allowed creation of databases of daily rainfall erosivity (DEIDB) and daily precipitation (DPDB). The RUSLE considers an event erosive if at least one of two conditions is true: i) the cumulative rainfall is greater than 12.7 mm, or ii) the cumulative rainfall has at least one peak greater than 6.35 mm in 15 min. Two consecutive events are considered different from each other if the cumulative rainfall in a period of 6 hr is less than 1.27 mm. In the present study we have considered all the rainfall events with precipitation above 0mm as erosive events. This threshold was used for calibrating the models; otherwise we could not do monthly calibration.

There was a need to adjust the original time series of erosive events to a daily time scale. Thus, if there were more than one erosive event in a given day their values were summed up to give a total daily erosivity. This involved some 2% of the original dataset composed by 66,486 events. In some rare cases an erosive event occurred during two or more consecutive days. In those cases—only 0.66% of all the erosive events—the event was assigned to the day with the highest precipitation. This procedure was preferred to splitting up the erosive event, which would have modified the rainfall erosivity value.

2.3. Rainfall erosivity estimates

2.3.1 RUSLE *R* factor

Daily EI_{30} values for the period 1997–2006 were calculated using rainfall intensity data recorded every 15 minutes, and the RUSLE model. The RUSLE model uses the Brown and Foster (1987) approach to calculating the average annual rainfall erosivity, R (MJ mm ha^{-1} h^{-1} y^{-1}):

$$R = \frac{1}{n}\sum_{j=1}^{n}\sum_{k=1}^{m_j}(EI_{30})_k \quad (1)$$

where n is the number of years of the record, m_j is the number of erosive events for a given year j, and EI_{30} is the rainfall erosivity index of a single event k. Thus, the R factor is the average value of the annual cumulative EI_{30} over a given period. An event's rainfall erosivity EI_{30} (MJ mm ha^{-1} h^{-1}) is calculated as follows:

$$EI = EI_{30} = \left(\sum_{r=1}^{o} e_r\, v_r\right) I_{30} \quad (2)$$

where e_r and v_r are, respectively, the unit rainfall energy (MJ ha^{-1} mm^{-1}) and the rainfall volume (mm) during a time period r, and I_{30} is the maximum rainfall intensity in a 30 min period during the event (mm h^{-1}). The unit rainfall energy (e_r) is calculated for each time interval as:

$$e_r = 0.29\ [1 - 0.72\exp(-0.05 i_r)] \quad (3)$$

where i_r is the rainfall intensity during the time interval (mm h^{-1}).

2.3.2 Rainfall erosivity estimates from daily rainfall intensity data

Model A: The Richardson et al. (1983) exponential model

Event rainfall erosivity values (EI) are usually well fitted to the event precipitation amount (P) by an exponential relationship (Richardson et al. 1983):

$$EI = a\,P^b + \varepsilon, \quad (4)$$

where *a* and *b* are empirical parameters and ε is a random, normally distributed error. The *R* factor, equal to the annual cumulative *EI*, is obtained by summing all event values. The parameters *a* and *b* can be adjusted month-by-month to take account of intra-annual variations in rainfall characteristics. This leads to the more general expression:

$$EI_m = a_m P^{b_m} + \varepsilon , \quad (5)$$

where $m = 1, 2, \ldots, 12$ represents the month of the year being evaluated. The exponential relationship has been applied to event (Richardson et al. 1983, Posch and Rekolainen 1993), daily (Bagarello and D'Asaro 1994) and even monthly data (Yu and Rosewell 1996a; Petkovsek and Mikos 2004). In all these studies parameter *a* was the only variable, and parameter *b* was assumed to be stationary across the year.

Parameter estimation in the Richardson et al. (1983) model is achieved by ordinary least squares (OLS) regression after a logarithmic transformation of the terms in equation (4). OLS regression offers an analytical solution to minimizing the sum of squared errors, SSE:

$$SSE_m = \sum_{m=1}^{M} (E_m - \hat{E}_m)^2 , \quad (6)$$

where E_m and $\hat{E}_m$ are the observed and predicted cumulative rainfall erosivity for month *m*, respectively, $\hat{E}_m$ is the predicted cumulative rainfall erosivity for the month, and *M* is the number of months for which data are available.

Model B: The Richardson et al. (1983) exponential model by weighted least squares

A problem with the method of Richardson et al. (1983) is that it tends to underestimate systematically the R factor values. This has been pointed out by a number of authors, and it has been usually attributed to the logarithmic transformation of the variables to allow parameter estimation by OLS (Richardson et al. 1983, Elsenbeer et al. 1993, Posch and Rekolainen 1993). However, we believe that the *R* factor is underestimated mainly because parameter estimation by OLS is based on minimizing the squared errors *at the daily or rainfall*

203 *event scale*, resulting in excessive significance being placed on many small events that do not
204 contribute materially to the cumulative annual erosivity. In fact, many studies have shown the
205 paramount importance of the contribution of very few, but intense, daily rainfall events to total
206 annual rainfall erosivity.

207 In order to avoid excessive influence of small erosive events during parameterization of the
208 Richardson et al. (1983) model, we have also tried an alternative parameterization method
209 based on weighted least squares regression (WLS). In WLS weights can be assigned to the
210 observations in order to modify their influence on the fitting process. In this case, the weights
211 w_i were computed as the inverse of the empirical frequency of the observations:

212 $$w_i = \left(\frac{i}{n}\right)^{-1}, \quad (7)$$

213 where i is the order of the observation after the series has been sorted in ascending order, and
214 n is the number of observations in the series.

215

216 *Model C: The Yu and Rosewell model*

217 Using the equation of Richardson et al. (1983) requires a logarithmic transformation of the
218 data, which usually leads to underestimation of erosivity and bias when the predicted values
219 are transformed back to the original scale (Richardson et al. 1983, Elsenbeer et al. 1993, Posch
220 and Rekolainen 1993). In addition, individual regression equations must be developed for each
221 month (Posch and Rekolainen 1993) or season (Richardson et al. 1983), resulting in a large
222 number of parameters. Yu and Rosewell (1996a) proposed an alternative equation based on
223 the Richardson et al. (1983) method, in which the seasonal variation of parameter a (termed α
224 in their study) was modeled parametrically using a periodic function:

225 $$EI = \alpha\left[1 + \eta\cos(2\pi\frac{1}{12}m - \omega)\right]P^{\beta} \quad \nabla P > P_0, \quad (8)$$

where η controls the amplitude of the intra-annual variation of α, and ω controls the phase, i.e. the month of the year for which the value of α is maximum. The periodic function modifying parameter α allows introduction of seasonal effects such as varying storm types, using a reduced number of parameters in comparison with the method of Richardson et al. (1983). Equation 6 is evaluated at the daily time scale, and only those values of daily rainfall greater than a threshold value P_0 are considered. A value of 0.0 mm is usually valid for P_0 when daily data are used. The parameter ω is kept constant, depending on the month registering the highest erosivity for a given rainfall amount.

To minimize bias in the estimated erosivity values, Yu and Rosewell (1996a) recommended using parameter estimates without data transformation. The adjustment between the observed and predicted values is done by using an iterative algorithm minimizing the sum of squared errors.

Model D: A modified Yu and Rosewell model

Application of the original model of Yu and Rosewell—Model C—only allows intra-annual variation of parameter α. An alternative model could allow periodic variation in parameter β, while parameter α is kept stationary:

$$EI = \alpha P^{\beta\left[1+\eta\cos(2\pi\frac{1}{12}m-\omega)\right]}. \quad (9)$$

Model E: The five-parameter modified Yu and Rosewell model

A logical extension of Model D would be to allow intra-annual variation in both α and β:

$$EI = \alpha\left[1+\eta_\alpha\cos(2\pi\frac{1}{12}m-\omega)\right]P^{\beta\left[1+\eta_\beta\cos(2\pi\frac{1}{12}m-\omega)\right]}, \quad (10)$$

where η_α and η_β control the amplitude of the variation of α and β, respectively. In the previous formulation the phase parameter ω is kept equal for both α and β. The parameters α, β, η_α and η_β were estimated by minimizing the sum of squared errors as described above.

Since equations (8), (9) and (10) are highly non-linear no analytical solution is available, and an iterative method has to be used for minimizing the SSE. In this case a genetic algorithm (*Pikaia*; Charbonneau 1995, Metcalfe and Charbonneau 2003) was used to determine the best values for parameters α, β, η_α and η_β, depending on the model. Parameter ω can be estimated directly from the observations as:

$$\omega = \frac{\pi}{6} m_{\max}, \tag{11}$$

where m_{max} is the month registering the highest average erosivity for the complete record period.

2.3.3 Rainfall erosivity estimates based on monthly precipitation and annual rainfall intensity indices

Other approaches exist to estimate rainfall erosivity without daily rainfall data. As a consequence of the relationship between rainfall erosivity and precipitation intensity, alternative ways to calculate the impact of rainfall on soil are based on the precipitation concentration, for example by applying the modified Fournier index, or by regression of the RUSLE *R* factor upon different precipitation intensity statistics calculated at the annual level.

Model F: Precipitation intensity indices

Annual rainfall erosivity has been related to several precipitation intensity indices calculated at the annual level (Table 1). A common indicator of high rainfall erosivity values is the mean annual precipitation (Renard and Freimund 1994). Several studies have highlighted the relationship between the *R* factor and occasional heavy rainfall events recorded during a year (Martínez-Casanovas et al. 2002, González-Hidalgo et al. 2007, Angulo-Martínez et al. 2009). Rainfall erosivity can also be related to several precipitation intensity indices that are also

correlated with the presence and duration of dry spells. Since there are many alternative indices to regress upon, it is wise to perform a multiple regression analysis to find an optimum estimator of the *R* index of the form:

$$R = b_0 + \sum_{1}^{n} b_n x_n + \varepsilon \quad (12)$$

where b_0–b_n are regression coefficients and x_1–x_n are independent variables.

For model selection (identification of the significant variables) in the present study we used a forward stepwise method based on the Akaike's information criterion (Venables and Ripley 2002). A ten-fold cross-validation procedure was used, which involved repeating the stepwise method ten times, each time omitting one-tenth of the sample from the analysis (Breiman and Spector 1992). In an ideal situation all ten repetitions should yield the same set of significant variables, indicating high reliability of the model. A robust regression procedure was used to avoid the excessive influence of outlier observations present in the data. This involved assigning to each observation a weight that was inversely proportional to its influence on the model fitting process (Marazzi 1993). The R statistical analysis package (R Development Core Team 2008) was used for the regression analysis.

Model G: The modified Fournier index

Estimation of the annual rainfall erosivity using the modified Fournier index has been proposed when only monthly precipitation data are available (Arnoldus 1977) i.e.:

$$MFI = \sum_{i=1}^{i=12} \frac{P_i^2}{P} \quad (13)$$

where P_i is the mean monthly precipitation of the month i and P is the mean annual precipitation. The relationship between *MFI* and the *R* factor showed better adjustment following an exponential distribution (Ferro et al. 1999). The *R* factor values can be estimated from the *MFI* using the following equation:

$$R = aMFI^{b} + \varepsilon, \quad (14)$$

where *a* and *b* are empirical parameters and ε is a random, normally distributed error.

The Fournier index has been used in several recent studies (Apaydin *et al*. 2006, Gabriels 2006). The application of this model yielded the following equation for the study area:

$$R = 21.56 MFI^{0.927}. \quad (15)$$

Model H: The F index (Ferro et al. 1991)

A modification in the *MFI* for estimating rainfall erosivity has been proposed by Ferro et al. (1991):

$$F_F = \frac{P}{12}\left[\frac{\sum_{j=1}^{N} P_j^{1+CV^2(p_{i,j})}}{\sum_{j=1}^{N} P_j}\right] = \sum K_i \frac{P}{12}, \quad (16)$$

where P_j is the annual rainfall amount of the year *j*, *CV* is the variation coefficient of the month *i* from the year *j*, K_i is a constant depending on the month *i*, and *P* is the mean annual rainfall of the study period

In this case, the value *K* is an indicator of the monthly rainfall distribution in the year. The best adjustment between F_F index and the *R* factor was achieved with an exponential distribution—i.e. eq. 14—(Ferro et al. 1999). In the study area the *R* factor values where obtained by using the following equation:

$$R = 0.0542\, F_F^{1.412} \quad (17)$$

2.5. Validation

The resulting rainfall erosivity prediction models were assessed using a set of validation statistics that compared the observed and estimated values of the *R* factor. We used a set of goodness-of-fit statistics (Table 2) including: i) the mean and the standard deviation of the predicted and observed values, as a measure of centrality and dispersion, and ii) the *NS*

coefficient of efficiency (Nash and Sutcliffe 1970), which indicates how close scatters of predicted values are to the line of best fit; this is similar to the coefficient of determination R^2, without being markedly affected by outlier data. This validation statistic is commonly used in rainfall erosivity studies (Yu et al. 2001, Petkovsek and Mikos 2004). In addition we used two error statistics: i) the mean bias error (*MBE*), which is centered around zero and is an indicator of prediction bias; and ii) the mean absolute error (*MAE*), which is a measure of the average error. We did not use the root mean square error (*RMSE*) because it is highly biased by outlier data, and it is difficult to discern whether it reflects the average error or the variability of the squared errors (Willmott and Matsuura 2005).The validity of the models was also evaluated by goodness-of fit plots and the comparison between the spatial distribution of the observed values and the spatial distribution of the *R* factor estimates from the different models. The *R* factor maps were obtained by spatial interpolation of the at-site points using smoothing splines for spatial interpolation.

3. Results

3.1 Spatial distribution of rainfall erosivity over the study area

A detailed spatial distribution of rainfall erosivity in the study area, as estimated using the RUSLE *R* factor, is shown in Figure 2. Overall, the spatial distribution of the *R* factor in the study area could be explained by the proximity to—or isolation from—the major water masses of the Cantabrian and the Mediterranean seas. The relief, with mountain ranges to the north, south, and east of the region, modifies this general pattern by increasing rainfall in those areas. Another effect of the relief is the isolation of the central area from main precipitation sources through creation of a rain shadow zone. All these influences result in a rather complex spatial pattern of erosivity.

A broad NW−SE gradient in the spatial distribution of the *R* factor could be detected, which was also evident in the monthly regimes. To confirm this observation, we analyzed the

monthly behavior of rainfall erosivity at the 111 stations by clustering all stations into three zones (Figure 3). The NW zone, which is influenced by the Atlantic Ocean, had the highest monthly rainfall values and minimum rainfall erosivity; the highest erosivity was attained at the beginning of summer. The central zone included the majority of stations. Here, the precipitation rates were less than in the NW zone (although still significant), but erosivity was greater and showed two annual peaks, one in late spring (May–June) and a second (the larger) at the end of summer (August–September). The NE zone has a typical Mediterranean rainfall distribution, with maxima in spring and autumn. The erosivity distribution was maximal in autumn. It is important to note that the spring rainfall peaks were not as erosive as those of the autumn, because of differences between these seasons in rainfall generation mechanisms. The rainfall recorded during the spring months came from several precipitation events of relatively low intensity. In contrast, the precipitation in autumn was usually attributable to a few very intense events.

3.2. Model A equation parameters

We have analyzed the *a* and *b* parameters calibrated monthly using the exponential relationship of Richardson et al. (1983) in eq. (5) above. As explained earlier, further development of this model was largely dependent on how seasonal variation of the *a* and *b* parameters was modeled.

As shown in Figure 3, rainfall erosivity displayed a very marked seasonal pattern that did not coincide with the seasonal variation in monthly precipitation. In principle, this is consistent with seasonal variation in the parameters of the exponential relationship. Figures 4 and 5 show the monthly distribution of parameters *a* and *b*. Differences between observatories were relatively small, and were usually noticed in the month during which maximum values were registered. Both parameters showed significant temporal variation within the year, following a periodic model. Minimum values were found in winter (December–January) and the maxima

376 at the end of summer (July–August). This result supports the validity of the models of Yu and
377 Rosewell (models C, D, and E).
378 Another noteworthy result is that both of the *a* and *b* parameters showed seasonal variation. As
379 mentioned above, many studies have minimized the influence of parameter *b* by holding *b*
380 constant throughout the year. This is because *b*, being an exponent, has a greater influence
381 than has parameter *a* on the estimations, and hence is much more sensitive to calibration
382 errors. However, our results show that both parameters varied significantly, supporting the
383 hypothesis that a model incorporating such variation could yield better results. In this context,
384 Figures 4 and 5 show that parameters *a* and *b* displayed very similar relative patterns, with
385 minima and maxima that occurred in the same months and that differed only in the magnitude
386 of variation. This supports the hypothesis that a model with one ω parameter, which controls
387 the phase of the periodic function, replacing both *a* and *b*, would be adequate (this is model E).
388

389 ### 3.3 Comparison between methods

390 #### 3.3.1 Models based on daily data

391 All the daily rainfall erosivity models yielded good results, as was made evident by the
392 validation statistics (table 5), goodness-of-fit plots (figure 6), and by checkingthe spatial
393 distribution of the *R* factor estimates (figure 7). The models based on the Yu and Rosewell
394 equations (models C, D, and E) were most satisfactory. Model C—the original Yu and
395 Rosewell (1996a) equation—ranked best among them. The exponential relationship model of
396 Richardson et al. (1983) fitted by the ordinary least squares method (model A) underestimated
397 rainfall erosivity, as evidenced by all the validation statistics. However, the Richardson et al.
398 (1983) model fitted by weighted least squares (Model B) showed better agreement, as
399 evidenced by the validation statistics and the goodness-of fit plots (table 5 and figure 6,
400 respectively). This result confirmed that the underestimation of model A, which has been
401 attributed to the logarithmic transformation applied to the data by a number of authors, is in

fact related to the utilization of a fitting algorithm that is sub-optimal for estimating the R factor, due the high importance of very few, but intense precipitation events.

Looking at the goodness-of-fit plots (figure 6), it is evident that model A resulted in significant under-estimation of the R factor, whereas model B provided better predictions. The models based on the Yu and Rosewell (1996a) equation, e.g. models C, D and E, had also a good agreement, although in general tended to over-estimate the R factor. Among the three parametric models the differences were narrow; the best overall fit was given by the Yu and Rosewell original model—model C—followed by model E.

With respect to goodness-of-fit and error statistics (Table 5), all models based on daily data (A, B, C, D, and E) gave good results. Overall, model A ranked lowest, underestimating both the mean and the standard deviation of rainfall erosivity, and showing the strongest bias of all methods. This model also had the lowest goodness-of-fit statistic (*NS*) of all models using daily data, and ranked closer to theoretically less refined methods, such as the regression method (model F). As a comparison, when using weighted least squares in the Richardson et al. (1983) model—Model B—better validation statistics were obtained.Among the models based on the equation of Yu and Rosewell (C, D, and E), model C was the best considering all the validation statistics altogether. Between models D and E, model E yielded the best results.

Finally, a comparison was made among the various methods in terms of the spatial distribution of rainfall erosivity (Figure 7). Based on these results we rejected models A and B which resulted in underestimation and a poor approximation to the observed values of rainfall erosivity (Figure 2). Differences between the others models were hardly noticed, and all adequately reproduced the observed spatial pattern (Figure 2). However, it must be noted that interpolation techniques may increase underestimation.

3.3.2 Models based on monthly or annual rainfall intensity indices

An exploratory correlation analysis (Table 3) showed that high and significant correlations existed between rainfall erosivity on the one hand, and several rainfall intensity indices computed on an annual basis, on the other. The highest correlation coefficients were found with R3GD and R5GD; these are the amounts of precipitation accumulated during the three and five wettest days, respectively, confirming the hypothesis that very few events are responsible for a large part of annual rainfall erosivity. The explanatory variables selected by the stepwise procedure were R5GD, WSM, and RS; the latter two figures are the maximum wet spell duration and the ratio between the average length of wet and dry spells (Table 4). It is notable that the regression analysis included two variables that did not show significant correlations with *R* when considered individually, although other indices that were probably highly correlated with R5GD were excluded. The selection of variables was remarkably constant during the jack-knife process, confirming the statistical significance of the three variables mentioned. In contrast, the correlations between the *R* factor and the modified Fournier index, and the *R* factor with the F_F index were very poor (Table 4), and yielded unsatisfactory results.

Figure 8 shows the goodness-of-fit plots for the three models. Underestimation occurred in all cases, particularly using the regression based on the Fourier index—model G. Among all models based on monthly or annual rainfall intensity indices model F yielded the best results, which were closer to those based on daily data and exponential relationships, although the values of all validation statistics were worse (table 5). Estimation by model H —regression based on the F_F index— showed better agreement than using the original Fournier index, but still model F ranked best.

The validation statistics (Table 5) showed that the MFI regression afforded the poorest performance of all methods tested and, particularly, resulted in a marked underestimation of the standard deviation of rainfall erosivity, as well as the highest absolute error and the worst *NS* statistic. The rainfall intensity indices regression model—model F—was relatively poor

compared to methods based on the Yu and Rosewell equation, although the validation statistics were almost as good as those for model A. Validation statistics obtained for Model H slightly improved those from Model G, but this model still ranked very low to be considered a valid choice when other models are affordable.

Finally, the spatial distribution of the estimated *R* factor values determined by these methods (Figure 9) matched the observed pattern quite well (Figure 3) in the case of model F, but was very poor when model G and H were employed. This fact was especially evident for the highest values recorded at the southeast part of the region. Those high values corresponded to an extreme event recorded at the daily scale which is still disguised at the monthly level.

4. Discussion and Conclusions

Estimation of rainfall erosivity is of great importance for soil erosion assessment, and has important implications for agriculture and land planning. Rainfall erosivity is an indicator of precipitation aggressiveness, and depends both on the rainfall energy (raindrop size distribution and kinetic energy) and the intensity of the storm event. Rainfall in Mediterranean climates is characterized by great temporal variability and high, brief, intensity (storms). This latter characteristic particularly affects rainfall erosivity, which increases with greater occurrence of few, very intense, events (González-Hidalgo et al. 2007).

In this study we used the RUSLE *R* factor, calculated employing high resolution (15 min) rainfall data, as an indicator of rainfall erosivity, and compared *R* factor values with estimates obtained using alternative methods based on daily precipitation data and precipitation indices calculated on monthly and annual scales. This comparison was conducted to identify valid, spatially-distributed estimates of rainfall erosivity using the type of rainfall data that are most usually available.

Among the methods used to estimate the RUSLE *R* factor, the Yu and Rosewell (1996a) equation and variations thereof (models C, D and E) yielded the best results, and the data were

consistent when tested using several statistical validation tools and by direct comparison of the maps of rainfall erosivity produced by each method. The main advantage of the Yu and Roswell method is that this approach allows investigators to reproduce seasonal variations in the relationship between daily precipitation and rainfall erosivity without a need to divide the data into monthly segments; this makes more efficient use of the information available. Although most previous studies assumed that the *b* coefficient remained constant throughout the year (Richardson et al. 1983, Bagarello and D'Asaro 1994, Petkovsek and Mikos 2004) our results demonstrate that both of the parameters *a* and *b* showed a periodic variation within the year. Moreover, the influence of parameter *b*, being an exponent, is greater than that of parameter *a*. This result drove directly to the proposal of two variants of the original model of Yu and Rosewell (1996a)—Models D and E. We compared three versions of the original model of Yu and Rosewell, in which only α, only β, or both α and β, were allowed to vary over the year by using a periodic function. Although the ability of the models to predict the *R* factor was supposed to increase with themodel complexity, the validation statistics did not allow such a clear conclusion to be drawn, since the original model of Yu and Rosewell (1996a) yielded results which were marginally better than the other two variants. Hence, even though there are strong theoretical evidences in favor of a model with both α and β parameters allowed varying, for practical use we have to recommend the simplest formulation with only α varying, that is, the original formulation of Yu and Rosewell (1996a). It is possible that a model with both parameters varying—model E—provides a better way to estimate the rainfall erosivity at a monthly or even a daily basis, although this hypothesis has not been tested in this work. Due to the high complexity and non-linearity of model E, it is also possible that better results be obtained by using fitting methods other than the genetic algorithm used in this work. These possibilities, however, would need further testing and are outside the scope of this work, which is restricted to predicting the RUSLE *R* factor.

504 In contrast, the method based on the exponential relationship of Richardson et al. (1983)
505 yielded unsatisfactory results, systematically underestimating the annual erosivity and the
506 variance thereof. This outcome has been reported on many occasions, and has been attributed
507 to the logarithmic transformation that is usually performed on the variables to allow parameter
508 estimation by the least squares method. However, our results demonstrate that under-
509 estimation of the R factor is caused by the sub-optimal character of the OLS algorithm. We
510 have shown that when the weighted least squares method was applied—Model B—the
511 underestimation was reduced very significantly. This fact confirmed that underestimation by
512 theOLS algorithm is due toexcessive significance being placed on many small events that do
513 not contribute materially to the cumulative annual erosivity expressed by the R factor. In fact,
514 the results of our analyses confirmed the paramount importance of the contribution of very
515 few, but intense, daily rainfall events to total annual rainfall erosivity.

516 In the absence of daily rainfall data, other ways to estimate the *R* factor are based on
517 regression upon intensity precipitation indices on monthly or annual scales. These are
518 commonly available statistics that are readily obtainable through any meteorological service.
519 Our results showed that the modified Fournier index or its modified form—the F_F index—are
520 not appropriate for estimating the *R* factor and result in severe underestimation.The best
521 alternative to using a daily-based approach was a multivariate linear model based on three
522 indices (the cumulative precipitation for the five days with most rain, the maximum wet spell
523 duration, and the ratio between the length of the average wet and dry spells).

524 The parameter values obtained from models A and B in this study are similar to those obtained
525 in several studies carried out in other Mediterranean areas (Bagarello and D'Asaro 1994,
526 Petkovsek and Mikos 2004, D'Asaro et al. 2007). All those studies developed regional models
527 based on exponential relationships upon daily rainfall amounts. One or more model
528 parameters were considered spatially invariant and were maintained equal for all the stations
529 in the study area. In this study we have preferred to perform an at-site analysis, i.e. calibrating

all the model parameters individually for each station. This was recommended due to the existence of contrasting rainfall regimes within the study area, and also because regional variations were found in the values of the parameters when fitted individually for each site

There remain inherent limitations in the use of daily weather records for estimating the rainfall erosivity term in the universal soil loss equation. Erosivity includes kinetic energy and intensity measures that are poorly represented by daily rainfall values (Selker et al. 1990). Future research may provide better calibration of the Brown and Foster (1987) rainfall kinetic energy equation by measuring natural rainfall properties in any particular region.

Acknowledgements

We thank the Ebro River Hydrographical Confederation (Confederación Hidrográfica del Ebro; CHE) for providing the data used in this study. The research of M.A. was supported by a JAE-Predoc Research Grant from the Spanish National Research Council (Consejo Superior de Investigaciones Científicas; CSIC).

References

Arnoldus, H.M.J., 1977. Methodology used to determine the maximum potential average annual soil loss due to sheet and rill erosion in Morocco. *FAO Soils Bulletin*, **34**: 39-51.

Angulo-Martínez, M., López-Vicente, M., Vicente-Serrano, S.M., Beguería, S., 2009. Mapping rainfall erosivity at a regional scale: a comparison of interpolation methods in the Ebro Basin (NE Spain). *Hydrology and Earth Systems Science*, (in press).

Apaydin, H., Erpul, G., Bayramin, I., Gabriels, D. 2006. Evaluation of indices for characterizing the distribution and concentration of precipitation: A case for the region of Southeastern Anatolia Project, Turkey. *Journal of Hydrology*, **328**, 726-732.

Bagarello, V., D'Asaro, F., 1994. Estimating single storm erosion index. *Transactions of the American Society of Agricultural Engineers*, 37, 3, 785-791.

Banasik, K., Górski, D., 1994. Rainfall erosivity for south-east Poland. *Conserving soil resources. European perspectives* (ed. Rickson), 201-207. Lectures in soil erosion control, Silsoe College, Cranfield University, UK.

Breiman, L., Spector, P. 1992. Submodel selection and evaluation in regression: The X-random case. *International Statistical Review*, **60**:291-319.

561 Brown, L.C., Foster, G.R., 1987. Storm erosivity using idealized intensity distributions.
562 *Transactions of the American Society of Agricultural Engineers*, **30**: 379-386.

563 Charbonneau, P. 1995. Genetic algorithms in astronomy and Astrophysics. *Astrophys. J. Supp.*
564 **101**. 309.

565 Creus, J., 2001. Las sequías en el valle del Ebro. *Causas y consecuencias de las sequías en*
566 *España*, A. Gil and A. Morales, Eds. Universidad D'Alacant, 231-259.

567 Cuadrat, J.M. 1991. Las sequías en el valle del Ebro. Aspectos climáticos y consecuencias
568 económicas. *Rev. Real Acad. Ciencias*, **85**: 537-545.

569 Curse, R., Flanagan, J., Frankenberger, B., Gelder, D., Herzmann, D., James, D., Krajenski,
570 W., Kraszewski, M., Laflen, J., Opsomer, J., Todey, D. 2006. Daily estimates of rainfall,
571 water runoff and soil erosion in Iowa. *Journal of soil and water conservation*, **61** (4):
572 191-199.

573 D'Asaro, F., D'Agostino, L., Bagarello, V. 2007. Assessing changes in rainfall erosivity in
574 Sicily Turing the twentieth century. *Hydrological processes*. DOI: 10.1002/hyp.6502

575 Diodato, N. 2004. Estimating RUSLE's rainfall factor in the parto of Italy with a
576 Mediterranean rainfall regime. *Hydrology and Earth System Sciences*, **8**(1): 103-107

577 Domínguez-Romero, L., Ayuso Muñoz, J.L., García Marín, A.P. 2007. Annual distribution of
578 rainfall erosivity in western Andalusia, southern Spain. *Journal of soil and water*
579 *conservation* **62** (6): 390-401.

580 Dunkerley, D. 2008. Rain event properties in nature and in rainfall simulation experiments: a
581 comparative review with recommendations for increasingly systematic study and
582 reporting. *Hydrological processes.* DOI: 10.1002/hyp.7045

583 Elsenbeer, H., Cassel, D.K., Tinner, W. 1993. A daily rainfall erosivity model for Western
584 Amazonia *Journal of Soil and Water Conservation*, **48**, 439-444.

585 Efron, B., Tibshirani, R.J. 1997. Improvements on cross-validation: the .632+ bootstrap
586 method," *J. of the American Statistical Association*, **92**, 548-560.

587 Ferro, V., Porto, P., Yu, B. 1999. A comparative study of rainfall erosivity estimation for
588 southern Italy and southeastern Australia, *Hydrological sciences journal*, **44**, 3-24.

589 Ferro, V., Giordano, G., Iovino, M. 1991. Isoerosivity and erosion risk map for Sicily,
590 *Hydrological sciences journal*, **36** (6), 549-564.

591 Gabriels, D. 2006. Assesing the Modified Fournier Index and the Precipitation Concentration
592 Index for some European countries. Boardman and Poesen (Ed.) *Soil Erosion in Europe*.
593 John Wiley & sons. 675-684.

594 García-Ruiz, J.M., Arnáez, J., White, S.M., Lorente, A., Beguería, S. 2000. Uncertainty
595 assessment in the predition of extreme rainfall events: an example from the Central
596 Spanish Pyrenees. *Hydrological Processes*, **14**: 887-898.

597 Garrido J, García JA. 1992. Periodic signals in Spanish monthly precipitation data. *Theoretical*
598 *and* 756 *Applied Climatology* **45**: 97–106.

599 González-Hidalgo, J.C., Peña-Monnè, J.L., de Luis, M. 2007. A review of daily soil erosion in
600 western Mediterranean areas. *Catena*, **71**: 193-199

601 Hoyos, N., Waylen, P.R., Jaramillo, A. 2005. Seasonal and spatial patterns of erosivity in a
602 tropical watershed of the Colombian Andes. *Journal of Hydrology*, **314:** 177-191.

603 Hudson, N., 1971. *Soil Conservation*. Cornell University Press, Ithaca.

Lal, R. 1976. Soil erosion on alfisols in Western Nigeria. III – Effects of rainfall characteristics. *Geoderma* **16**: 389-401

Lana X, Burgueño A. 1998. Spatial and temporal characterization of annual extreme droughts in Catalonia (Northeast Spain). *International Journal of Climatology* **18**: 93–110.

Lasanta, T. 2003. Gestión agrícola y erosión del suelo en la cuenca del Ebro: el estado de la cuestión. *Zubía*, **21**: 76-96.

Llasat, M.C., Barriendos, M., Barrera, A., Rigo, T. 2005. Floods in Catalonia (NE Spain) since the 14th century. In Benito, G, Ouarda, T.B.M.J., Bárdossy, A (Eds.) Palaeofloods, hystorical data & climate variability: Applications in flood risk assessment. *Journal of Hydrology*, **313** (1-2): 32-47.

Llasat, M.C. 2001. An objective classification of rainfall events on the basis of their convective features: Application to rainfall intensity in the northeast of Spain. *International Journal of Climatology*, **21**: 1385-1400

Marazzi, A. 1993. *Algorithms, Routines and S Functions for Robust Statistics*. Wadsworth & Brooks/Cole.

Martínez-Casanovas, J.A., Ramos, M.C., Ribes-Dasi, M. 2002. Soil erosion caused by extreme rainfall events: mapping and quantification in agricultural plots from very detailed digital elevation models. *Geoderma*, **105:** 125-140.

Martín-Vide, J. 1994. Diez características de la pluviometría española decisivas en el control de la demanda y el uso del agua. *Boletín de la AGE*., **18**: 9-16.

Metcalfe, T.S., Charbonneau, P. 2003. Stellar structure modelling using a parallel genetic algorithm for objective global optimization. *Journal of computational physics*, **185**, 176-193.

Nash, J.E., Sutcliffe, J.V., 1970. River flow forecasting through conceptual models part I – A discussion of principles. *Journal of Hydrology*, **10**, 282-290.

Onori, F., De Bonis, P. Grauso, S. 2006: Soil erosion prediction at the basin scale using the revised universal soil loss equation (RUSLE) in a catchment of Sicily (southern Italy). *Environmental Geology*, **50**: 1129-1140. DOI: 10.1007/S00254-006-0286-1.

Peñarrocha D, Estrela, MJ, Millán M. 2002. Classification of daily rainfall patterns in a Mediterranean area with extreme intensity levels: the Valencia region. *International Journal of Climatology* **22**: 677–695.

Petkovsek, G., Mikos, M. 2004. Estimating the R factor from daily rainfall data in the sub-Mediterranean climate of southwest Slovenia. *Hydrological sciences journal*, **49** (5): 869-877.

Posch, M., Rekolainen, S. 1993. Erosivity factor in the Universal Soil Loss Equation estimated from Finnish rainfall data. *Agricultural Science in Finland*, **2**, 271-279

R Development Core Team, 2008. *R: A Language and Environment for Statistical Computing*. Vienna (Austria), R Foundation for Statistical Computing

Renard, K.G., Foster, G.R., Weesies, G.A., McCool, D.K., Yoder, D.C., 1997. *Predicting Soil Erosion by Water: A Guide to Conservation Planning with the Revised Universal Soil Loss Equation (RUSLE).* Handbook #703. US Department of Agriculture, Washington, DC.

Renard, K.G., Freimund, J.R., 1994. Using monthly precipitation data to estimate the R factor in the revised USLE. *Journal of hydrology*, **157** (1-4): 287-306.

Richardson, C.W., Foster, G.R., Wright, D.A., 1983. Estimation of Erosion Index from Daily Rainfall Amount. *Transactions of the American Society of Agricultural Engineers*, 26, 153-160.

Romero, R., Guijarro, J.A., Ramis, C. and Alonso, S. 1998. A 30-year (1964-1993) daily rainfall data base for the Spanish Mediterranean regions: first exploratory study. *International Journal of Climatology*, **18**: 541-560

Selker, J.S., Haith, D.A., Reynolds, J.E., 1990. Calibration and testing of Daily Rainfall Erosivity Model. *Transactions of ASAE*, **33**, 1612-1618.

Shi, Z.H., Cai, C.F., Ding, S.W., Wang, T.W., Chow, T.L., 2004. Soil conservation planning at the small watershed level using RUSLE with GIS. *Catena*, **55**: 33-48

Van der Knijff, J.M., Jones, R.J.A., Montanarella, L., 2000. *Soil Erosion Risk Assessment in Italy*. European Commission— European Soil Bureau. 52 pp.

Venables, W. N., Ripley, B. D. 2002. *Modern Applied Statistics with S.* Fourth edition. Springer.

Vicente-Serrano, S.M. 2005. *Las sequías climáticas en el valle medio del Ebro: factores atmosféricos, evolución temporal y variabilidad espacial*. Publicaciones del Consejo de Protección de la Naturaleza de Aragón, 277p.

Willmott CJ, Matsuura K. 2005. Advantages of the mean absolute error (MAE) over the root mean square error (RMSE) in assessing average model performance. *Climate Research* **30**: 79–82.

Wischmeier, W.H., 1959. A rainfall erosion index for a universal soil-loss equation. *Soil Science Society of America Proceedings* , **23**: 246-249.

Wischmeier, W.H., Smith, D.D., 1978. Predicting rainfall erosion losses: a guide to conservation planning. *USDA Handbook 537*, Washington, DC.

Yu, B., Hashim, G.M., Eusof, Z., 2001. Estimating the R-factor with limited rainfall data: a case study from peninsular Malaysia. *Journal of Soil and Water Conservation*, **56**: 101-105

Yu, B., Rosewell, C.J., 1996a. An assessment of daily rainfall erosivity model for New South Wales. *Australian Journal of Soil Research (Aust. J. Soil Res.)*, **34**, 139-152

Yu, B., Rosewell, C.J., 1996b. A robust estimator of the *R* factor for the Universal Soil Loss Equation. *Trans. ASAE*, **39**, 559-561

Yu, B., Rosewell, C.J., 1996c. Rainfall erosivity estimation using daily rainfall amounts for South Australia. *Australian Journal of Soil Research (Aust. J. Soil Res.)*, **34**, 721-733

682 Figure Captions
683
684 **Figure 1.** Location of the study area and the precipitation observatories of the SAIH network.
685 As it is part of a hydrological warning and control system, the SAIH network is not evenly
686 distributed; more importance is placed on headwater areas at the borders of the study area.
687 However, this distribution coincides with the spatial variation of rainfall characteristics, which
688 shows small spatial variance in the center of the Ebro Basin and maximum spatial variance
689 towards its margins.
690 **Figure 2.** Spatial distribution of the RUSLE *R* factor in the Ebro Basin.
691 **Figure 3.** Monthly distribution of rainfall erosivity (RUSLE *R* factor) and precipitation in the
692 Ebro Basin.
693 **Figure 4.** Monthly distribution among the analyzed observatories for parameter *a* from the
694 Richardson et al. (1983) exponential relationship.
695 **Figure 5.** Monthly distribution among the analyzed observatories for parameter *b* from the
696 Richardson *et al*. (1983) exponential relationship.
697 **Figure 6.** Comparison between observed *R* values (ordinate axis) and those estimated by
698 various methods (abscissa axis): A) model A; B) model B; C) model C; D) model D; and E)
699 model E. Line of best fit (continuous diagonal line), and regression line (dashed).
700 **Figure 7.** Spatial distribution of estimated *R* values by: A) model A; B) model B; C) model C;
701 D) model D and E) model E; . These maps can be compared to Figure 2.
702 **Figure 8.** Comparison between observed *R* values (ordinate axis) and those estimated by
703 various methods (abscissa axis): F) model F; G) model G; and H) model H. Line of best fit
704 (continuous diagonal line), and regression line (dashed).
705 **Figure 9.** Spatial distribution of estimated *R* values by: F) model F; G) model G; and H)
706 model H.
707

708 Table 1. Acronyms and definition of the selected indices from the daily precipitation series.

Acronym	Definition	Units
P	Total precipitation	mm
WD	Number of wet days (precipitation >1mm)	days
PI	Simple daily intensity (P/WD)	mm
C90	Annual 90th percentile	mm
R90N	Nº of events with precipitation greater than long-term 90th percentile (P90)	days
R90T	Percentage of total precipitation from events above P95	%
C95	Annual 95th percentile	mm
R95N	Nº of events with precipitation greater than long-term 90th percentile (P95)	days
R95T	Percentage of total precipitation from events above P95	%
C99	Annual 99th percentile	mm
R99N	Nº of events with precipitation greater than long-term 90th percentile (P99)	days
R99T	Percentage of total precipitation from events above P99	%
R1GD	Greatest day total precipitation	mm
R3GD	Greatest 3-day total precipitation	mm
R5GD	Greatest 5-day total precipitation	mm
R7GD	Greatest 7-day total precipitation	mm
R9GD	Greatest 9-day total precipitation	mm
R11GD	Greatest 11-day total precipitation	mm
R13GD	Greatest 13-day total precipitation	mm
R15GD	Greatest 15-day total precipitation	mm
R17GD	Greatest 17-day total precipitation	mm
R19GD	Greatest 19-day total precipitation	mm
R21GD	Greatest 21-day total precipitation	mm
WSM	Max nº of consecutive wet days (precipitation >1mm)	days
DSM	Max nº of consecutive dry days (precipitation <1mm)	days
WS	Average Max nº of consecutive wet days (precipitation >1mm)	days
DS	Average Max nº of consecutive dry days (precipitation <1mm)	days
RS	Ratio (WS/DS)	

709

710

711 Table 2. Error statistics.

Statistical criteria	Definitions:
	N : nº of observations O : observed R value $\bar{O}$: mean of obs. R values P: predicted R value $P_i' = P_i - \bar{O}$ $O_i' = O_i - \bar{O}$
Mean bias error (MBE)	$MBE = N^{-1} \sum_{i=1}^{N} (P_i - O_i)$
Mean absolute error (MAE)	$MBE = N^{-1} \sum_{i=1}^{N} \lvert P_i - O_i \rvert$
Efficiency Coefficient	$NS = 1 - \frac{\sum_{i=1}^{N} (O_i - P_i)^2}{\sum_{i=1}^{N} (P_i - P_m)^2}$

712

713

714

715 Table 3. Correlation coefficients between the observed *R* factor and several precipitation intensity indices. See
716 Table 1 for definition of the indices.

P	WD	PI	C90	R90N	R90T	C95
0.50*	0.042	0.79*	0.76*	0.047	0.18	0.80*
R95N	R95T	C99	R99N	R99T	R1GD	R3GD
0.036	0.19	0.80*	0.056	0.26*	0.79*	0.84*
R5GD	R7GD	R9GD	R11GD	R13GD	R15GD	R17GD
0.84*	0.82*	0.80*	0.79*	0.77*	0.75*	0.74*
R19GD	R21GD	WSM	DSM	WS	DS	RS
0.72*	0.71*	0.0068	0.10	0.094	0.049	0.044

717 * significant at the confidence level α=0.05

718

719 Table 4. Regression coefficients and variance, and regression analysis for the precipitation intensity indices (see
720 Table 1) and the modified Fournier index (MFI).

Explanatory variables	r^2	Variables selected
Regression against precipitation intensity indices based on daily data	0.727	R5GD, WSM, RS
Modified Fournier Index	0.250	---
F_F index	0.408	---

721

722

Table 5. Accuracy measurements for the *R* factor models: means and standard deviations of the observed and predicted values.

	Mean	Standard dev.	*MBE*	*MAE*	*NS*
Observed	903.9	619.91	---	---	---
Model A	708.2	573.5	-194.4	205.9	0.745
Model B	774.8	628.5	-128.4	152.8	0.839
Model C	969.8	696.4	64.9	97.6	0.947
Model D	1000.2	729.3	95.0	132.4	0.909
Model E	998.2	697.9	93.0	124.5	0.910
Model F	1025.9	530.2	120.8	243.2	0.574
Model G	805.4	320.4	-97.6	329.6	-1.903
Model H	830.1	392.6	-73.2	293.6	-0.512

Figure 1

Click here to download high resolution image

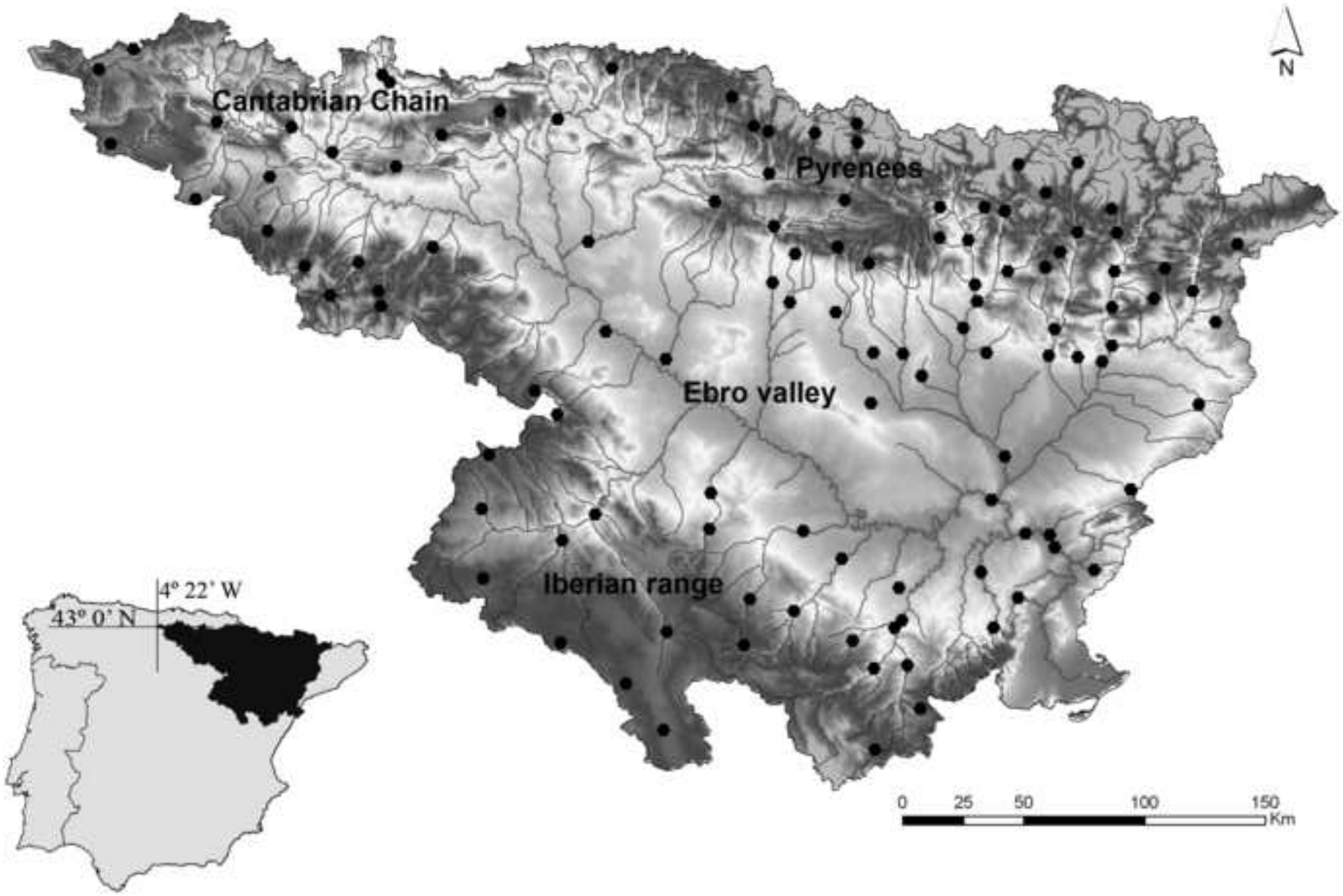

Figure 2

Click here to download high resolution image

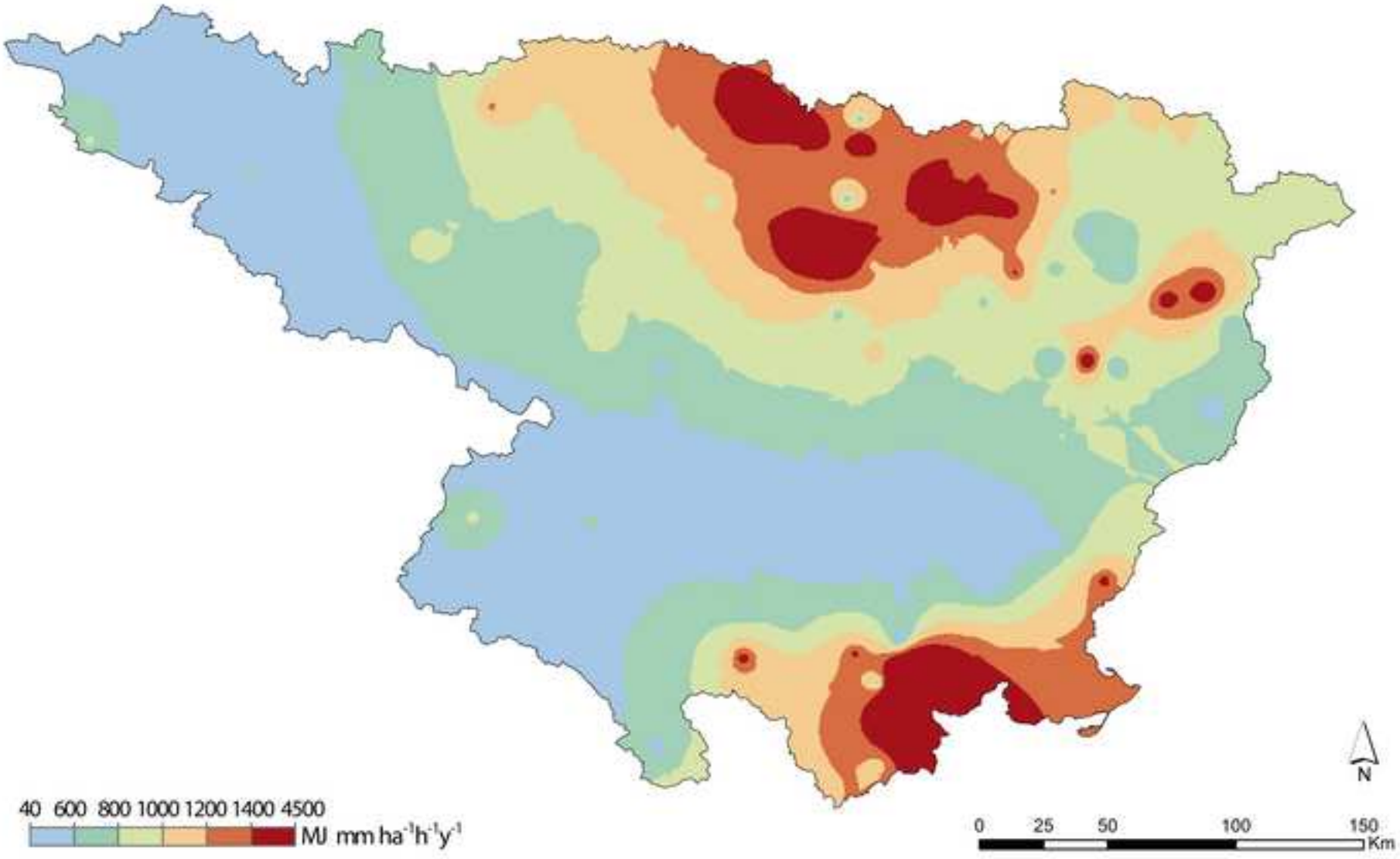

Figure 3

Click here to download high resolution image

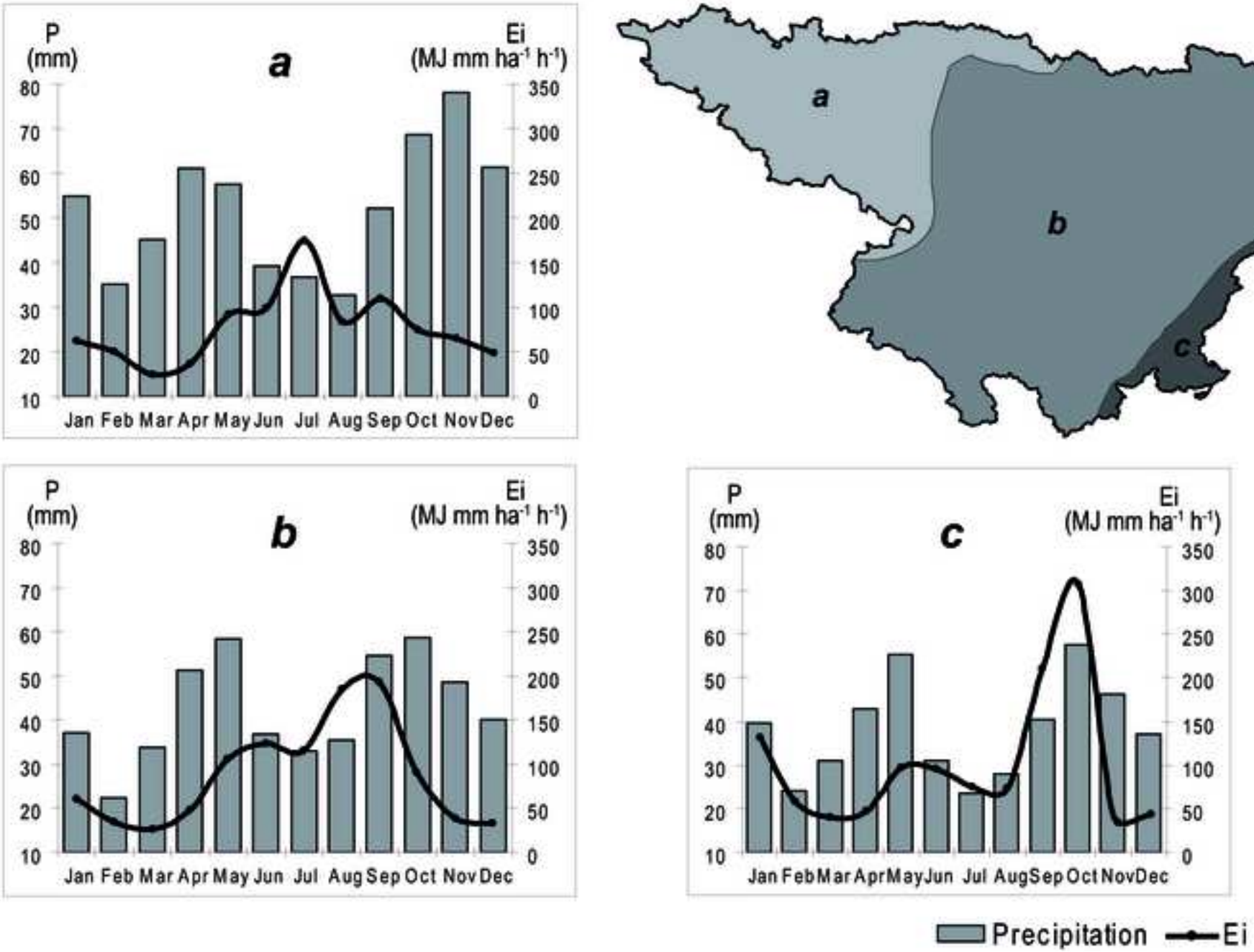

Figure 4

Click here to download high resolution image

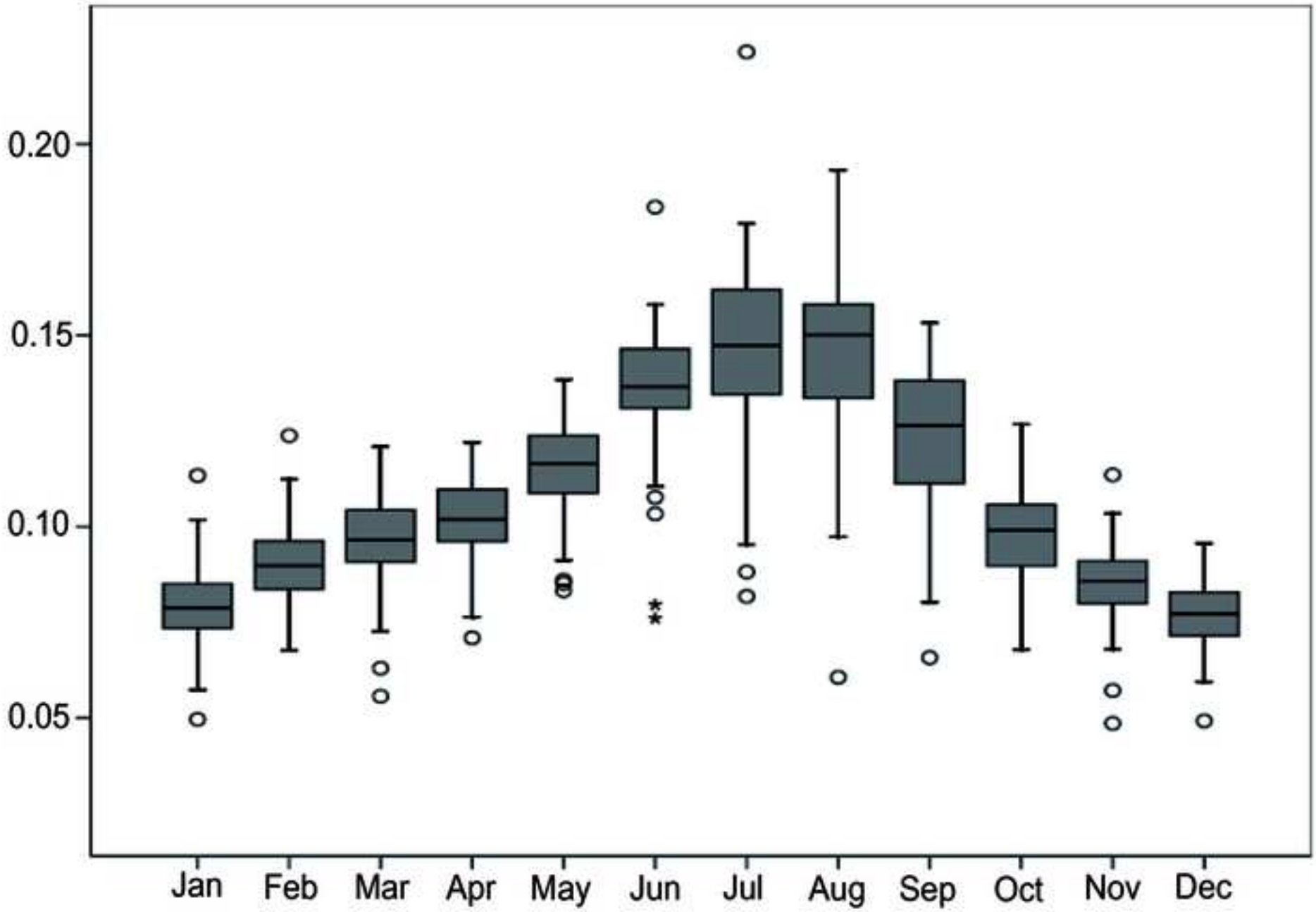

Figure 5

Click here to download high resolution image

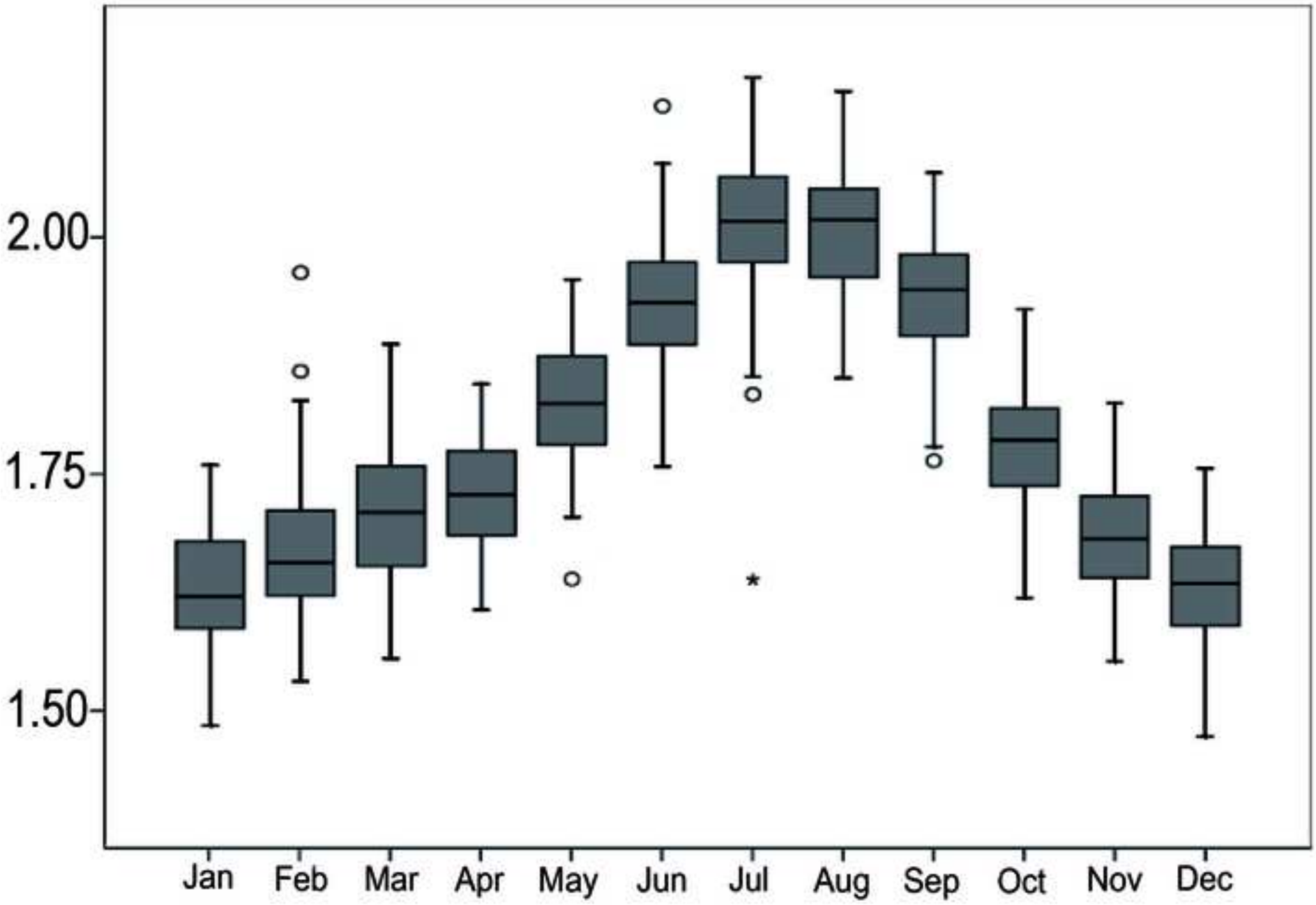

Figure 6

Click here to download high resolution image

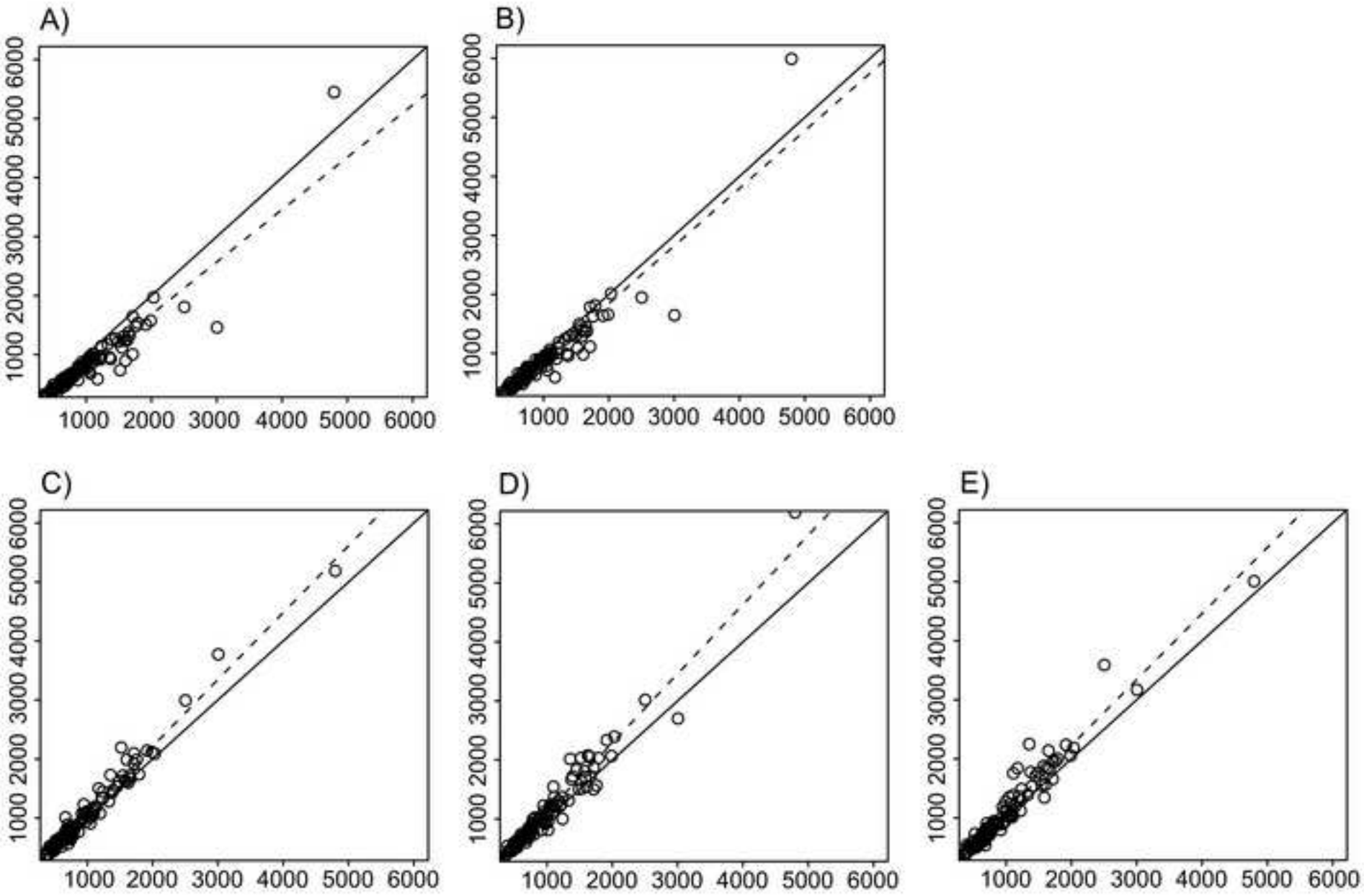

Figure 7

Click here to download high resolution image

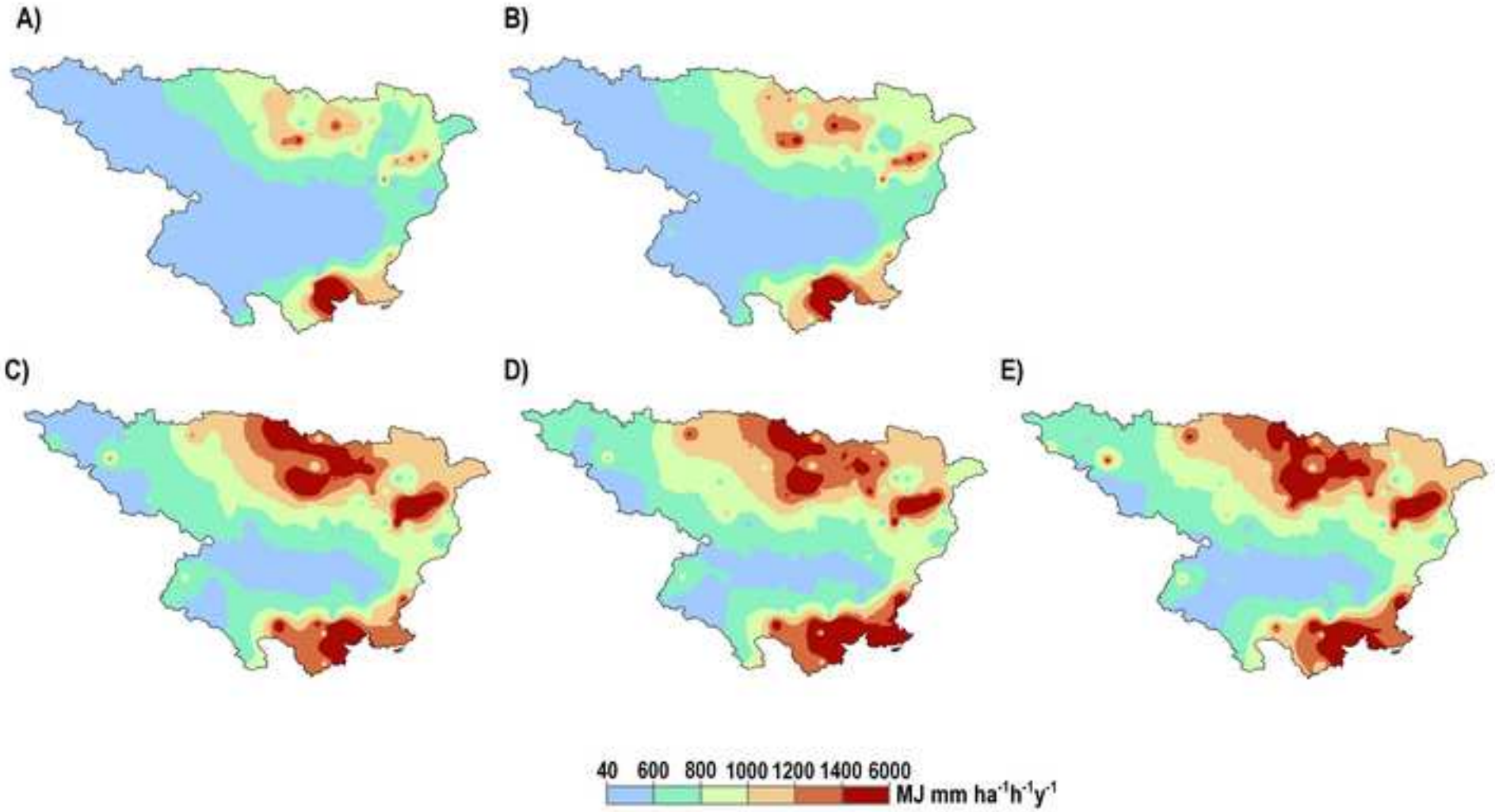

Figure 8

Click here to download high resolution image

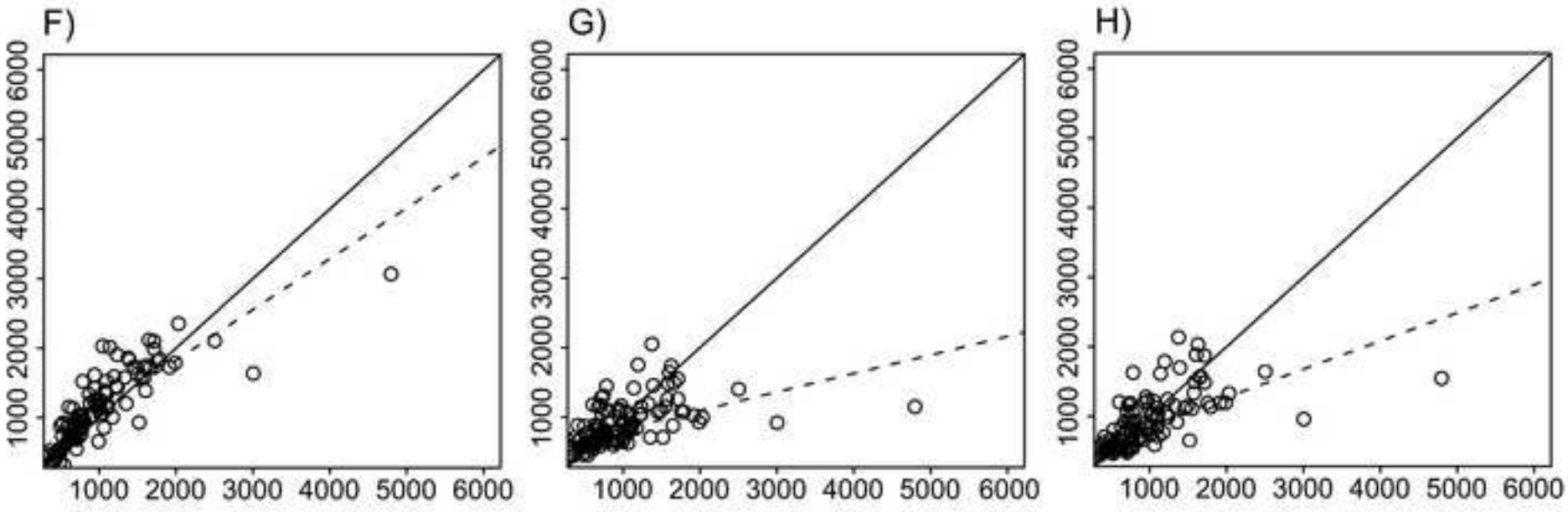

Figure 9

Click here to download high resolution image